Structure and function of the UVDE repair protein

Paspaleva, K.

Chapter

1

General introduction Damage recognition in DNA repair systems

1. INTRODUCTION

DNA carries genetic information essential for all processes of life. The DNA in all living organisms is under a constant attack by numerous endogenous and environmental agents.

1.1 Endogenous DNA damaging sources

At physiological conditions DNA continuously interacts with oxygen and water, which can lead to creation of DNA lesions. Major sites of oxidative and hydrolytic damage are the amino groups of cytosine, adenine and guanine. The loss of the amino groups (deamination) occurs spontaneously and converts affected DNA bases into uracil, hypoxanthine and xanthine, respectively. Another target for the hydrolytic and oxydative sources is the N-glycosylic bond. Cleavage of this bond results in a base loss and creation of an apurinic/apyrimidinic (AP) site in the DNA. The pyrimidine nucleotides are considerably more stable than the purine ones, since cytosines and thymines are lost at a much lower rate, compared to the adenines and the guanines (Lindahl and Nyberg, 1974). Other well known DNA damaging agents are reactive oxygen species (ROS), which include oxygen ions, free radicals and peroxides. ROS can be formed as a by-product of the cellular metabolism or induced by exogenous sources such as ionizing radiation. One of the most potent ROS is the hydroxyl radical (•OH). It targets the double bonds of DNA bases as well as the deoxyribose sugars, from which it abstracts hydrogen atoms. The •OH attack on the double bond of thymine bases yields a 6-hydroxythymine radical, which can react with O_2, forming a thymine glycol (Demple and Linn, 1982). The •OH interactions with the DNA sugar residues may result in DNA fragmentation, base loss or strand breaks.

1.2 Exogenous DNA damaging sources

Exogenous (environmental) sources include ionizing radiation, cross-linking agents, alkylating agents and aromatic compounds. One of the most common natural sources for induction of DNA lesions is the UV component of sunlight.

UV light

Depending on its wavelength, UV irradiation has been divided into: UVA (320 to 400 nm), UVB (295 to 320 nm) and UVC (100 to 295 nm). Solar UV light, which reaches Earth, consists mainly of UVA and UVB, since UVC is efficiently blocked by the ozone layer.

The ultraviolet light can be absorbed by two adjacent pyrimidines in the DNA (Yoon *et al*., 2000), creating covalent bonds between them. Two common UV products are the cyclobutane pyrimidine dimer (CPD) and the 6-4 photoproduct (Figure 1).

The cyclobutane pyrimidine dimer is a four membered ring structure, formed between the C-5 and C-6 atoms of two neighbouring pyrimidines. T-T dimers (thymine dimers) are the most abundant of CPDs, although C-T, T-C and C-C dimers are also possible (Mitchell *et al*., 1992). Twelve isomeric forms of T-T CPDs exist, however, only two with the conformations *cis-syn* and *trans-cyn* occur with significant yields (David, 2001). The 6-4 Photoproduct (6-4PP) or also designated as pyrimidine-pyrimidone (6-4) photoproduct (Figure 1) is formed between C-6 of the 5' pyrimidine and C-4 of the 3' pyrimidine. Irradiation of the 6-4PP with 300-350 nm light converts it to a Dewar isomer (Figure 1), lesion that might be of a considerable biological relevance, since solar UV-B is in that wavelength range (Mitchel and Narin, 1989), (Taylor *et al*., 1988).

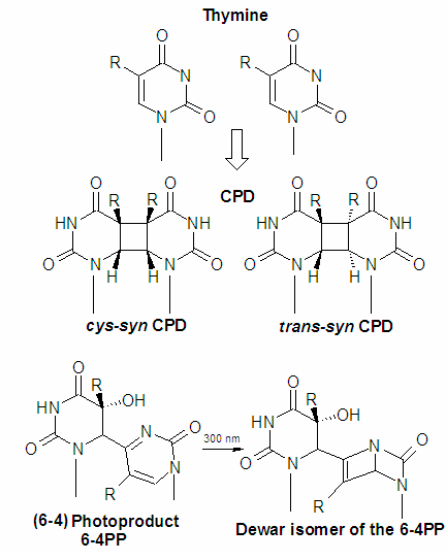

Figure 1. Structure of *cys-syn* and *trans-syn* cyclobutane pyrimidine dimer (CPD), (6-4) pyrimidone photoproduct (6-4PP) and its Dewar isomer. R represents a -CH_3 group.

It was shown (Yoon *et al*., 2000) that the frequency of occurrence of the CPD dimer is much higher (70 % - 80 %) than the induction of the 6-4PP (20 % - 30 %). However, the 6-4PP was revealed to be extremely mutagenic in contrast to the CPD (Mitchel and Narin, 1989). The CPD and the 6-4PP lesions are produced efficiently by UVC and UVB irradiation of DNA. The absorption of UVA photons by DNA is rather weak and it is thought that indirect mechanisms are responsible for its biological effects. The DNA damage induced by UVA may involve endogenous chromophores serving as radiation-absorbing intermediates. These can generate reactive oxygen species (ROS), which may further damage DNA (Friedberg *et al*., 2005).

The CPD and the 6-4PP exhibit significant differences in the DNA structural distortion. For the CPD different degree of helix deformation has been reported in literature. The bending induced by this lesion was initially reported as 30° by a circularization assay (Husain *et al*., 1988), but later as 7° in a phased multimer gel electrophoretic assay (Wang and Taylor, 1991). The CPD-containing DNA duplexes have also been a subject of theoretical studies (Pearlman *et al*., 1985), which predicted that CPD might cause bending from 6° up to 28° (Liu *et al*., 2000). More recently, the crystal structure of a DNA decamer containing a *cis-syn* thymine dimer showed 30° bending and 9° unwinding (Park *et al*., 2000). Incorporation of a *cis–syn* CPD into double-stranded DNA was also shown to destabilise the duplex by 1.5 kcal/mol (Jing *et al*., 1998). Although a reasonable Watson and Crick base pairing can still occur at the 3'T of the TT dimer, the base pairing of the 5'T is severely weakened (Park *et al*., 2000).

The 6-4PP causes 44° bending and a much higher degree of distortion compared to the CPD. The DNA duplex is destabilised by 6 kcal/mol and although initially it was reported that both pyrimidines of the 6-4PP loose their ability to form hydrogen bonds with the opposite strand (Mitchel and Narin, 1989), later NMR studies suggested that this happens only at the 3'-side of the (6-4) lesion (Kim and Choi, 1995).

The Dewar isomer induces a substantially different change in the overall DNA structure compared to the 6-4PP: for example an overall helical bending of 21° rather than the 44° caused by the 6-4PP (Lee *et al*., 1998).

DNA damages interfere with important processes like transcription and replication. Organisms cannot tolerate such genome threats and a variety of repair strategies have evolved to remove UV- and other DNA lesions (Wilson and Thomson, 1997). Four important pathways for repair of damaged bases in the DNA are: direct reversal, base excision repair (BER), nucleotide excision repair (NER) and UV damage endonuclease (UVDE) repair.

2. DIRECT REVERSAL

An example of simple and effective type of DNA repair is direct reversal. It involves damage specific enzymes, which restore the DNA to its native state in a single-step reaction. Such a simple pathway is kinetically faster than the multistep reaction, catalysed by multiprotein complexes

and is considered to be essentially error free (Friedberg *et al*., 2005). Here two examples of direct reversal will be discussed: the enzymatic removal of alkyl groups from the DNA by methyl transferases and the splitting of the UV induced CPD and 6-4PP by photolyases.

2.1 Methyl-transferases

The DNA repair protein O^6-alkylguanine-DNA alkyltransferase (AT) plays an important role in the cellular defence against alkylating agents. Alkyl adducts at the O^6-position of guanine are one of the most mutagenic lesions, although they are a relatively minor product in relation to other sites of DNA alkylation (Sedgwick *et al*., 2007), (Jackson *et al*., 1997).

Alkyltransferases (AT) act to remove alkyl groups from the O^6-position of a guanine through irreversible, single-step transfer of adducts to an active site cysteine residue (Samson, 1992), (Demple *et al*., 1985). In addition, AT can also remove the alkyl group from the O^4-position of an O^4-methylthymine (Paalman *et al*., 1997). The O^4-methylthymine is a rather rare methylation product, which can form an incorrect pair with guanine, resulting in a TA to CG transition (Sedgwick *et al*., 2007). Upon alkylation of the active site cysteine, the AT enzymes become highly susceptible to proteolysis (Kanugula *et al*., 1998) and therefore are called suicide proteins.

The O^6-alkylguanine-DNA alkyltransferase enzymes can be found in both eukaryotic and prokaryotic organisms and all proteins exhibit the same active site sequence V(I)PCHRV(I) (Friedberg *et al*., 2005). The best characterised AT proteins are those from *Escherichia coli* and man. *E. coli* contains two alkyl transferases: the product of the *ogt* gene and the product of the *ada* gene. The Ogt protein is constitutively expressed and preferentially removes bulky alkyl adducts such as O^6-benzylguanine (Goodtzova *et al*., 1997). In contrast, the *ada* gene is activated upon exposure to alkylating agents and the Ada enzyme is specialised in the repair of O^6-methylguanine. The crystal structure of the 19 kDa C-terminal domain of the *E. coli* protein (Ada-C) has been determined (Moore *et al*., 1994). This 178 amino acids C-terminal fragment is thought to be responsible for the methyltransferase activity on O^6-methyl-guanine-DNA. It houses a guanine specific binding pocket, in which, as predicted by DNA modelling, the methylated nucleotide can only bind if it is flipped out of the helix (Moore *et al*., 1994). So far the only co-crystal structure of an O^6-alkylguanine-DNA alkyltransferase bound to its substrate is available for the human homologue. The 21 kDa human protein (hAT) is homologous to the C-terminal domain of the Ada protein from *E. coli* (Ada-C). The structure of the hAT enzyme bound to its substrate (Daniels *et al*., 2004) elucidates the mechanism of damage verification and activity of this class of enzymes. Binding of the protein recognition helix widens the DNA minor groove and Arg128, situated at its beginning, promotes flipping of the target nucleotide out of the base stack into the hAT active site (Figure 2).

The arginine side chain stacks between the bases that flank the substrate nucleotide and can form a hydrogen bond with the orphaned cytosine, thus largely compensating for the loss of the nucleotide from the base stack. This ‘arginine finger’ stabilises the extrahelical DNA conformation and may also actively push nucleotides from the base stack during the DNA scanning (Daniels *et al*., 2004).

Figure 2. Crystal structure of the human O^6-alkylguanine-DNA alkyltransferase (hAT) bound to an O^6-methylguanine.

The extrahelical O^6-methylguanine and the Arg finger are indicated in blue.

Upon flipping, the extrahelical base is accommodated in a hydrophobic pocket, which provides geometric exclusion for all DNA bases, except guanine. Furthermore, hydrogen bonds are formed between the carbonyl groups of Cys145, Val148 and the amino group of a normal or methylated guanine, thus providing the enzyme selectivity for these bases. From the crystal structure, however, it is not entirely clear how hAT discriminates between the unmodified and the methylated guanine. It is currently thought (Daniels *et al*., 2004) that the difference in affinity for O^6-methylguanine over guanine is based solely on the larger hydrophobic surface derived from alkylation.

The next step in the hAT repair mechanism is the deprotonation of the active site cysteine. In this process (Figure 3), His146 acts as water-mediated general base to deprotonate Cys145, which serves as nucleophile in the dealkylation reaction. Donation of a hydrogen bond from Tyr114 to N3 of the target guanine may also promote the reaction by reducing the negative charge on the methylated guanine (Figure 3).

The crystal structure of the hAT enzyme reveals the presence of one Zn^{2+} ion. The metal ion lies in close proximity to the active site but is ~ 20 Å away from the reactive cysteine. The role of the Zn^{2+} is proposed to be structural, since it stabilises the interface between the N- and the C-terminal domains of the protein (Daniels *et al*., 2004).

In conclusion, the hAT enzyme does not utilize a metal cofactor for the deprotonation of the active site cysteine. Instead, as discussed, protein side chain (His146) acts as a water-mediated base and assists the deprotonation of Cys145.

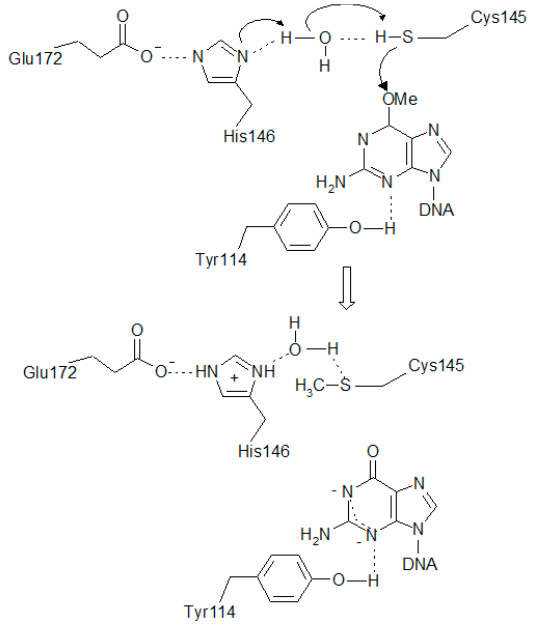

Figure 3. Reaction mechanism of the human AT alkyltransferase.

2.2 Photoreactivation

Photoreactivation is an efficient light-dependent process, which uses UVA (320 - 400 nm) and blue light (400 - 500 nm) to monomerise CPD dimers and 6-4 photoproducts. Photolyases are widely spread in nature and are monomeric proteins with molecular masses in the 53 - 66 kDa range, depending on the organism (Weber, 2005). Photolyases are distinguished by their different substrate specificity: CPD photolyase binds and repairs only CPD lesions, while the (6-4) photolyase reverses only the 6-4PP (Todo, 1999). All known photolyases contain non-covalently bound flavin adenine dinucleotide (FAD) as redox-active cofactor and an antenna pigment, which may differ (Zhao *et al*., 1997).

Photolyases can be found in various organisms: bacteria, yeast, insects and many vertebrates, including aplacental mammals. Some species like *Drosophila melanogaster* contain both a CPD and a (6-4) photolyase, however, most organisms posses only one type of photolyase (Goosen and Moolenaar, 2007). Although all placental mammals do not have any photolyase activity, two genes with a high similarity to the *Drosophila* (6-4) photolyase have been identified in the human genome and designated as hCRY1 and hCRY2 (Kobayashi *et al*., 1998). They do not have a DNA repair function, but instead, act as photoreceptors of the circadian clock. CRY genes were initially identified in the plant *Arabidopsis thaliana* and the gene products named CRY1 and CRY2 from 'cryptochrome'. CRY1 is involved in the plant elongation, while CRY2 regulates the flowering in response to blue light (Guo *et al*., 1998).

CPD photolyases

CPD photolyases are the best studied type of DNA photolyases and have been divided into two classes (I and II), based on their amino acid sequence similarity. Class I photolyases are found in many microorganisms, while most of class II photolyases are found in higher eukaryotes (Yasui *et al*., 2001). Recently, a CPD photolyase specific for CPD in ssDNA has been reported in *Vibrio cholerae* and designated as Cry1. Cry1 is a member of the Cry-DASH subfamily of cryptochromes and contains MTHF and FADH as chromophores (Worthington *et al*., 2003).

CPD photolyases generally have two kinds of chromophores. One is catalytic cofactor ($FADH_2$), which directly interacts with the CPD substrate in a photo-repair reaction. The other is light-harvesting cofactor, which acts as an antenna to harvest light, transferring the energy to the catalytic cofactor (Kim *et al*., 1992 and 2001). Class I photolyases are categorised according to their second chromophore into either a deazaflavin- or a folate-type. A deazaflavin-type photolyase has an 8-hydroxy-5-deazaflavin (8-HDF) as light-harvesting cofactor, while the folate-type photolyase has 5, 10-methenyltetrahydrofolic acid (MTHF) (Figure 4).

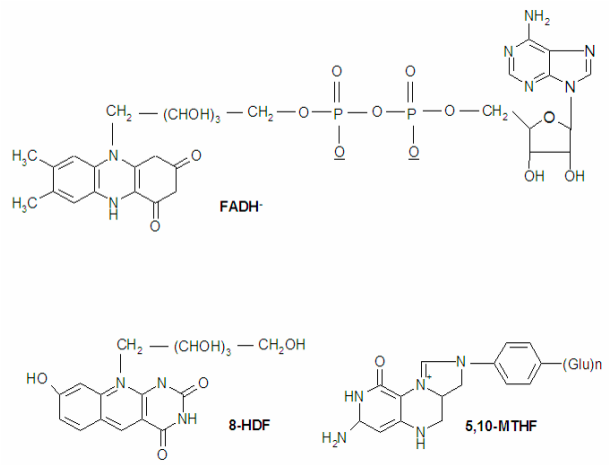

Figure 4. Structures of chromophores found in the pyrimidine dimer-DNA photolyases.

The folate class of DNA photolyases contains $FADH^-$ and 5,10-MTHF. The dezaflavin class of DNA photolyases contains $FADH^-$ and 8-HDF.

The recognition of CPD lesions by the DNA photolyases is elucidated by the crystal structure of the protein from *Anacystis nidulans* (Figure 5) in a complex with 14-nucleotide oligomer DNA duplex with a CPD in a central position (Mees *et al*., 2004). The structure is solved with 1.8 Å resolution. Despite the extensive structural distortion of the DNA upon photolyase binding, the protein itself undergoes only minor changes. The CPD lesion is flipped (Figure 5A) and inserted into the active site of the enzyme in such a way that the thymine dimer is suitably positioned to form hydrogen bonds with the catalytic $FADH^-$ (Figure 5B).

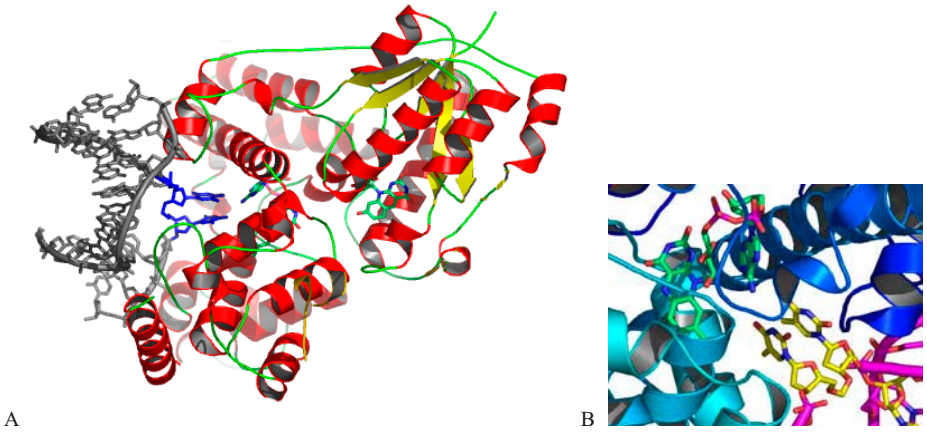

A B

Figure 5. The *A. nidulans* CPD photolyase in a complex with CPD containing DNA substrate.

A. The *A. nidulans* CPD photolyase-DNA complex. The CPD dimer (blue) is flipped out of the DNA helix.

B. Zoom in the enzyme active site. The flipped CPD lesion (yellow) is situated in close proximity to the $FADH^{\cdot}$ (colored green).

Salt bridges and hydrogen bonds are extensively formed along the protein surface and the phosphates of the DNA substrate. The crucial role of these interactions for the formation of the photolyase-CPD DNA complex is underlined by a mutation of a conserved arginine (*A. nidulans* R350 and *E. coli* R342), which forms direct and water-mediated hydrogen bonds with the O^2 and O^4 oxygens of the thymine bases (Essen *et al*., 2006). The arginine to alanine substitution is found to exhibit a severe phenotype causing a 32-fold decrease in the protein-DNA complexes and drop in activity from 98 % to about 60 %.

In the co-crystal structure of the CPD photolyase from *A. nidulans* the DNA is bend to about 50° and partially unwound. Residues Gly397 to Phe406 of the protein occupy the vacant space. The adenines complementary to the CPD are distorted, but still in an intrahelical position (Mees *et al*., 2004).

In summary, upon damage recognition the CPD photolyase flips the CPD lesion into its active site, where the DNA repair occurs by light-driven transfer of an electron from the excited $FADH^{\cdot *}$ to the CPD lesion (Figure 6). About 125 kJ/mol of the 240 kJ/mol of energy that is captured upon photon absorption is consumed during this initial electron transfer step (Carell *et al*., 2001). After electron capture, the splitting of the CPD lesion proceeds rapidly within 0.6 ns (Sancar, 2000). After DNA repair, the thymine pair has to flip back into the duplex DNA to form hydrogen bonds with the complementary adenines. This relaxation of the DNA backbone proceeds at a much lower speed than the repair of the CPD lesion itself, as was shown by spectroscopy methods (Essen *et al*., 2006).

(6-4) photolyases

The fact that both the CPD and the 6-4PP photolyases use FAD for catalytic factor suggests that the basic repair mechanism of both groups might be similar. In both cases electron donation is needed in order to convert the TT dimers (CPD or 6-4PP) to its original form. For the 6-4PP, however, this process is more complicated. The 6-4 photoproduct is structurally different from the cyclobutane pyrimidine dimer (CPD), since it involves creation of a bond between the C-6 of the 5' base and the C-4 of the 3' base (Figure 1). If an enzyme would break the 6-4 C–C bond the bases would not be restored to their original forms.

A (6-4) photolyase was described for the first time in *Drosophila melanogaster* (Todo *et al*., 1996), and later on, similar activity was observed in some vertebrates and plants. Currently, the cDNAs of (6-4) photolyase have been cloned from *D. melanogaster* (Todo *et al*., 1996), *Xenopus laevis* (Todo *et al*., 1997), *Arabidopsis thaliana* (Nakajima *et al*., 1998) and *Danio rerio* (Zebra fish) (Kobayashi *et al*., 2000). A crystal structure of a (6-4) photolyase with its 6-4PP substrate is not yet available.

Mutational analysis done on the *X. laevis* (6-4) photolyase (Hitomi *et al*., 2001) outlined three residues that are likely to be involved in the enzyme catalytic function. His354, Leu355 and His358 are highly conserved and computer modelling of the enzyme active site predicted them to be in a close contact with the 6-4PP damage. The model used the available structural data from the CPD photolyases in order to predict the possible organisation of the (6 - 4) photolyase active site. Based on the computer modelling, a catalytic mechanism was proposed (Hitomi *et al*., 2001) (Figure 7) in which His354 and His358 form hydrogen bonds with the N^3 atom of the 3'-pyrimidone and the hydroxyl group on the 5'-pyrimidine, respectively. While His358 abstracts a proton from the –OH group of the 5'-base, His354 protonates the N^3 of the 3'-base to generate a highly electrophilic iminium ion (Figure 7). Upon formation of the iminium ion, the reaction proceeds to formation of an oxetane intermediate. The intermediate is then converted to the native thymines by first absorbtion of excitation energy (from FADH) and later transfer of an electron back to the flavin radical (Hitomi *et al*., 2001).

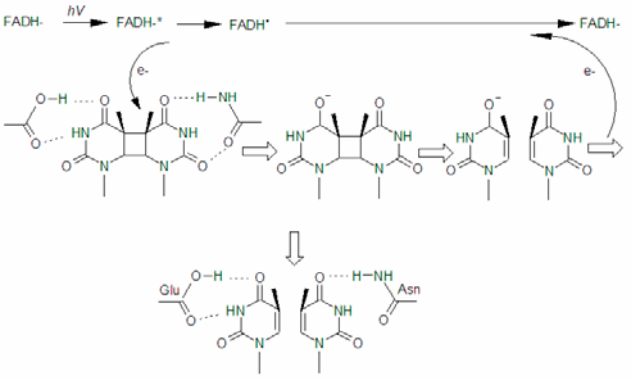

Figure 6. Reaction mechanism of the CPD photolyase from *A. nidulans*.

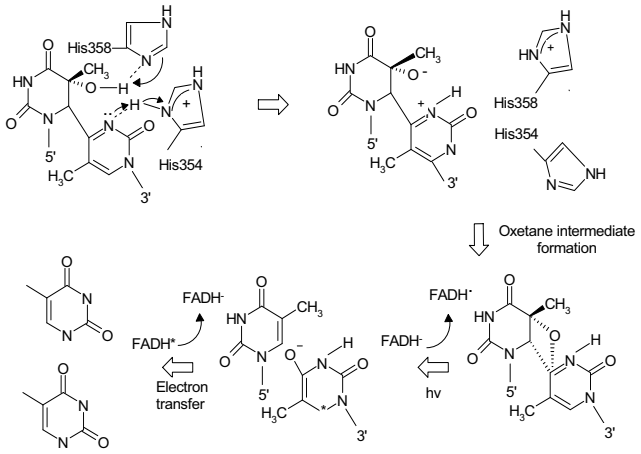

Figure 7. Proposed in literature mechanism for the 6-4PP photolyases activity.

3. NUCLEOPHILIC SUBSTITUTION: A COMMON MECHANISM FOR DNA HYDROLYSIS

All direct reversal DNA repair processes have a common problem – they can only repair alterations of the DNA bases. What organisms need are more general mechanisms, capable of correcting numerous lesions by removing the damaged nucleotides from the DNA backbone. This requirement is met by the excision repair pathways (Base Excision Repair and Nucleotide Excision Repair). A general feature in all excision repair mechanisms is the removal of the nucleotides containing the damage by incision of the DNA backbone.

The mechanism of a DNA cleavage is referred to as Nucleophilic substitution and the general reaction can be given as:

$$OH^- + LG\text{-}DNA \rightarrow (OH\text{-}LG\text{-}DNA) \rightarrow OH\text{-}DNA + LG:$$

First, the electron-rich nucleophile (OH^-) attacks the DNA backbone and forms an intermediate product (OH-DNA-LG). In this intermediate LG designates the so called leaving group, which at the collapse of the unstable intermediate, departs with an electron pair (LG:). Since the addition of the nucleophile and the elimination of the leaving group take place simultaneously (Carey and Sundberg, 2000), the nucleophilic substitution of DNA is classified as an S_N2 reaction (Jencks, 1981).

At a physiological pH, the DNA backbone has a large barrier for cleavage (Galburt and Stoddard, 2002), since it is negatively charged and electrostatically repels potential attacking nucleophiles (Westheimer, 1987). In order for the energy barrier to be overcomed and the DNA to be cleaved, several elements are required. These include a nucleophilic group (OH^-)

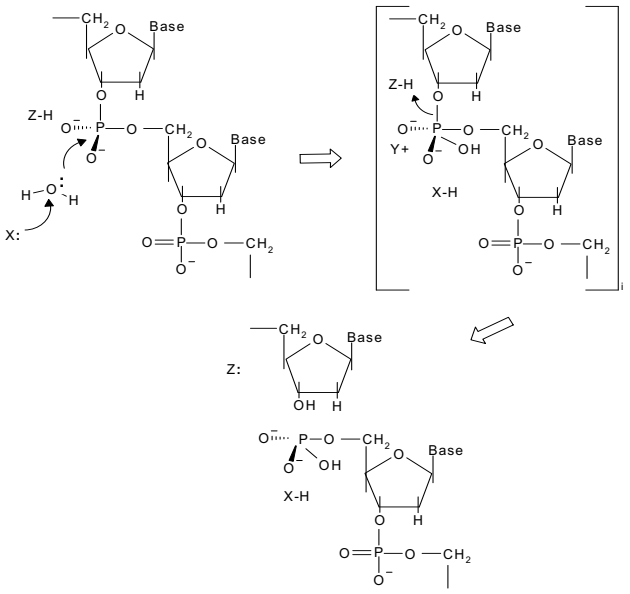

Figure 8. Schematic representation of the DNA cleavage performed by nucleases.

X represents a general base, Y represents a Lewis acid, Z-H represents a general acid, i and the brackets show the pentacoordinate intermediate, which is unstable.

to attack the DNA backbone, a basic moiety to activate and position the nucleophile (X in the scheme, Figure 8), a general acid to protonate the leaving group (Z-H) and the presence of one or more positively charged groups to stabilise the transition state (Galburt and Stoddard, 2002) (Figure 8). The role of a general base can be fulfilled both by metal cofactors and/or protein side chains. Divalent metal ions can also serve as Lewis acids (Y in the scheme), stabilizing the pentacoordinate intermediate.

One of the most relevant nucleophiles in the enzyme catalysis is the hydroxide ion (OH^-) and in order to produce it from water, enzymes generally use one or more metal cofactors. The pK_a of a water molecule coordinated to one or more divalent metal ions is reduced, thereby generating a hydroxide ion in close proximity to the protein active site (Gerlt, 1993 and 1992). Moreover, the DNA coordination to one or more divalent metal ions reduces or even eliminates the electrostatic repulsion between the water derived nucleophile and the negatively charged DNA backbone (Galburt and Stoddard, 2002), (Figure 8). Upon the OH^- attack, an OH-DNA pentacoordinate intermediate is formed (Guthrie, 1997). Creation and stabilisation of this intermediate within the nucleases' active site permits the enzymatic reaction to greatly exceed in speed compared to non-enzymatic reactions, where stabilisation of such intermediates is not possible (Jencks, 1981).

Endonucleases have been described to require one, two or three bound metals per active site. Exceptions are some ribonucleases, which cleave the phosphodiester bonds in RNA. They

do not use metal ions as cofactors, but instead utilize only protein side chains to provide the necessary positive charges, and to act as proton donors and acceptors (Fersht, 1999). Possible explanation for the lack of metals in some ribonucleolytic active sites could be the relative instability of the RNA phosphodiester bond, as compared to that of the DNA. And in that regard RNA cleaving enzymes have an easier job than the DNA nucleases (Galburt and Stoddard, 2002).

3.1 Endonucleases and one, two or three metal ion catalysis

Three metal ions mechanism

Three metal ions coordination has been described for the BER enzyme Endonuclease IV (Hosfield *et al*., 1999) and suggested as being part of the UVDE repair mechanism (Paspaleva *et al*., 2007). Endonuclease IV uses a cluster of Zn^{2+} ions, while UVDE most likely utilizes three Mn^{2+} ions. Classically, the three metal ion mechanism proceeds as follows: the metal ion in site I facilitates the formation of the nucleophilic hydroxide, whereas the metal ions in site II and III contribute mainly to stabilisation of the transition state and assist the leaving group. A detailed scheme of the Endo IV repair mechanism and the involvement of the Zn^{2+} cluster in the DNA cleavage can be found in chapter 4.2 of this introduction.

Two metal ions mechanism

Two metal ions catalysis has been described for the restriction enzymes *Bam*HI (Ca^{2+}) (Viadiu and Aggarwal, 1998), *Bgl*I (Ca^{2+}) (Newman *et al*., 1998) and *Pvu*II (Ca^{2+}) (Horton and Cheng, 2000). One of the metal ions was shown to be responsible for lowering the pK_a of a neighbouring water molecule, facilitating its deprotonation. Both metal ions are required to stabilise the transition state: one interacts with the oxygen of the OH^- nucleophile, and the other with the leaving group (Pingoud *et al*., 2005). As seen in the crystal structures of *Bam*HI, *Bgl*I and *Pvu*II, protein side chains assist the activation of the catalytic water and in that regard the presence of a third divalent metal ion is no longer needed.

One metal ion mechanism

Enzymes can even use only one metal ion for their DNA cleaving function. One-metal ion catalysis has been described for the restriction nucleases: *Eco*RI (Mn^{2+}) (McClarin *et al*., 1986), *Eco*O109I (Mn^{2+}) and *Hinc*II (Ca^{2+}) (Etzkorn and Horton, 2004). For all these nucleases the DNA hydrolysis reaction starts with the binding of a water molecule to the metal ion near the active site, resulting in its suitable positioning for the subsequent nucleophilic attack of the phosphorus atom. The water molecule is polarised through its coordination to the divalent metal ion coordination to the divalent metal ion, but mainly to protein side chains.

In summary, a number of nucleases utilize metal ions for their catalytic mechanism. The most commonly used divalent metal ions are Mg^{2+}, Mn^{2+}, Ca^{2+} and to lesser extend Zn^{2+}, Cu^{2+} and

Co^{2+} (Pingoud *et al*., 2005). Although the different nucleases might vary in respect to how many divalent metal ions are required for the hydrolysis of the DNA phosphodiester backbone, the underlying mechanism is the same. The divalent ions activate the nucleophilic water molecule and/or serve as efficient cofactors to stabilise the pentacoordinate transition state.

4. BASE EXCISION REPAIR

Base Excision Repair (BER) is a cellular mechanism, which targets a large variety of alterations of the DNA bases (Wilson and Thompson, 1997). The first step of BER involves removal of the modified base from the deoxyribose by DNA glycosylase. DNA glycosylases bind specifically to a target base and hydrolyse the N-glycosylic bond, releasing the damaged base, while keeping the DNA backbone intact. This step is referred to as damage specific, since each DNA glycosylase recognises one type of base alteration. Upon the glycosylase activity, an apurinic/apyrimidinic site is formed, which is substrate for AP-endonucleases. In the damage-general step of BER AP endonuclease cleaves the phosphodiester backbone 5' to the abasic site, resulting in the formation of a 3'-hydroxyl and 5' abasic sugar phosphate. The 5' abasic sugar phosphate is then removed with the help of exonuclease, or by specific DNA-deoxyribophosphodiesterase (dRpase). The sequential action of DNA glycosylases, AP endonucleases and exonucleases result in the creation of single nucleotide gap, which is filled by DNA polymerase and finally the resulting nick is sealed by DNA ligase.

A number of DNA glycosylases also possess DNA lyase activity, which in contrast to the AP endonucleases involves cleavage of the DNA backbone 3' to the AP-site. The activity of the combined glycosylases/lyases also results in creation of a single nucleotide gap, which can be filled by a DNA polymerase and sealed by a ligase.

4.1 Glycosylases

Uracil-DNA glycosylase

A Uracil in DNA is a result of cytosine deamination or can be product of dUTP incorporation. It is specifically removed by Uracil-DNA Glycosylase (UDG), which catalyses the hydrolysis of the N-glycosylic bond between the uracil (U) and the DNA sugar, leaving an AP site. UDGs are widely distributed small monomeric proteins (Friedberg *et al*., 2005). They classically do not require metal cofactors for their activity, although the DNA binding of some UDGs is strongly stimulated by Mg^{2+} ions (Kavli *et al*., 2002).

E. coli UDG is the founding representative of the class 1 UDG enzymes (Lindahl, 1974). The members of this family are able to remove uracil bases from both single and double strand DNA. Crystal structures are available for several members of the class 1 UDG family, including the *E. coli* homologue. The structure of *E. coli* UDG (Pearl, 2000) revealed an α/β fold, with a central four stranded β sheet. The co-crystal with an uracil containing DNA (Parikh *et al*.,

2000) (Figure 9) elucidated the *E. coli* UDG damage recognition mechanism. The enzyme was seen to kink the DNA at the lesion site and flip the abnormal nucleotide into an uracil specific pocket, where catalysis takes place. The shape of the pocket provides selection against purines. Furthermore, a tyrosine residue (Tyr66) blocks the accommodation of 5-methylated pyrimidines (thymines). A conserved asparagine (Asn123) assists in discrimination between cytosine and uracil by forming hydrogen bonds only with uracil.

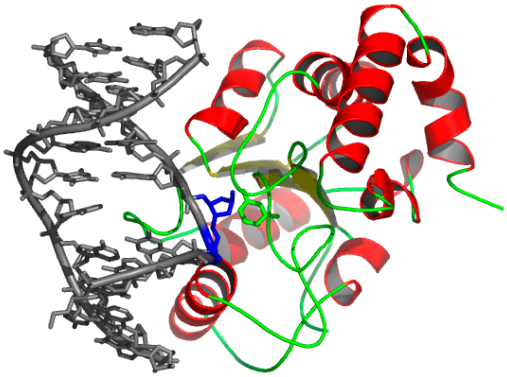

Figure 9. Structure of the *E. coli* Uracil-DNA glycosylase after hydrolysis of the N-glycosylic bond.

The uracil base is colored in green and the abasic site is shown in blue.

DNA glycosylases catalyse the nucleophilic displacement of a damaged base from the DNA using a water derived hydroxyl group. The reaction catalysed by the *E. coli* UDG involves the utilisation of Asp64 as a general base, which activates the water molecule for the subsequent attack of the N-glycosyl bond (Drohat *et al*., 1999). In addition, the closely located His187 assists in the electrostatic stabilisation of the uracil in the intermediate reaction phase. Since both the nucleophile creation and the intermediate stabilisation are performed by the UDG protein side chains, there is no actual need for divalent metal cofactors, which in other enzymes have been described to perform the same role.

T4 DNA glycosylase (T4 endo V)

The bacteriophage T4 encodes an enzyme for the specific removal of CPDs from the DNA. T4 endo V is 18 kDa *cis-syn* cyclobutane pyrimidine dimer specific glycosylase, with an additional AP lyase activity (Minton *et al*., 1975). The enzyme cleaves the N-glycosyl bond of the 5'-pyrimidine of the dimer and has no requirements for divalent cations or other cofactors (Friedberg *et al*., 1971). Upon the N-glycosyl bond cleavage, T4 endo V incises the DNA backbone 3' to the abasic site (lyase activity).

The T4 endonuclease V has been also shown to cleave the *trans-syn* CPD in a double-stranded DNA at a significant rate, although at least 100 times slower than the *cis-syn* dimer (Smith and Taylor, 1993).

Homologues of T4 endo V have been found in a limited number of eubacteria: in some *Prochlorococcus marinus* strains, *Brucella*, *Bordetella* as well as in *Sinorhizobium medicae* and *Pasteurella multocida* (Goosen and Moolenaar, 2007).

The X-ray crystal structures of the T4 endo V wild type (Morikawa *et al*., 1992) and a mutant (Nakabeppu *et al*., 1982) protein have been determined. The wild type T4 endo V is seen as a single domain structure of three α-helices, with the amino terminal region situated between helix one (H1) and helix three (H3), and in close proximity to the proposed catalytic residue (Glu23). The region accommodating Glu23 and the N-terminal Thr2 (Met1 is removed from the enzyme *in vivo*), which acts as the active site nucleophile is positioned in the centre of a groove, with dimensions just large enough to accommodate a single strand form of the DNA (Morikawa *et al*., 1992). The structures of three catalytically inactive mutants (E23Q, E23D, and R3Q) show an almost identical peptide backbone structure to the wild type.

A 2.75 Å co-crystal structure of an inactive T4-endonuclease V mutant (E23Q) with pyrimidine dimer-containing DNA duplex has also been determined (Golan *et al*., 2006). The structure of the enzyme is remarkably unchanged in the co-crystal and the DNA is bent at the dimer site by 60° (Figure 10). Upon DNA binding, the active site residues: Glu23 and the N-terminal Thr2 α-amino group protrude into the DNA stack.

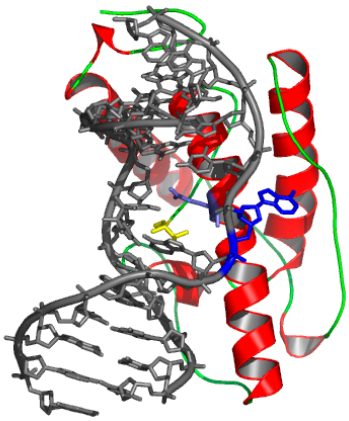

Figure 10. Structure of T4 endo V with DNA.

The N-terminal α-amino group, which acts as the active site nucleophile is colored in yellow. Glu23 is shown in violet and the flipped out adenine, opposite the scissile base, in blue.

There is no direct contact of the enzyme with the thymines of the pyrimidine dimer, but there are extensive interactions between protein side chains and the deformed DNA backbone,

near the dimer site. The Glu23 carboxyl side chain is positioned near the sugar, and the Thr2 α-amino group is close to the 5' thymine of the CPD, correctly positioned to act as the nucleophile in the glycosylase reaction. The adenine opposite the target thymine in the photodimer is flipped out of the DNA structure and bound into a pocket on the side of the enzyme. The adenine in the pocket does not form hydrogen bonds with any protein residues, suggesting that the major forces holding the adenine in place are relatively non-specific van der Waals interactions. However, some protein residues do assist in the stabilisation of the flipped conformation, since the extrahelical adenine is seen to be stacked between Tyr21 and Arg22.

Upon cleavage of the N-glycosylic bond of the 5'T of the CPD dimer, the T4 endo V catalyses a β-elimination reaction that cleaves DNA on the 3' side of the CPD (Vassylyev *et al*., 1995). Mutational studies showed that the main residue responsible for the enzyme AP lyase activity is Glu23, since mutation in this amino acid completely abolishes the DNA lyase activity (Hori *et al*., 1993).

4.2 AP endonucleases

AP endonucleases are metalloenzymes introducing a nick directly 5' to an AP site, as part of the second step of BER. They are ubiquitous and here only selected examples of well characterised AP endonucleases will be described.

Endonuclease IV (Nfo) family of AP endonucleas es

Nfo (endonuclease IV) is an endonuclease, which nicks AP sites in *E. coli*. The AP sites are cleaved directly 5′ to the lesion, leaving a hydroxyl group at the 3′ terminus and a deoxyribose 5′-phosphate at the 5′ terminus (Ljungquist, 1977). Endonuclease IV was shown not only to

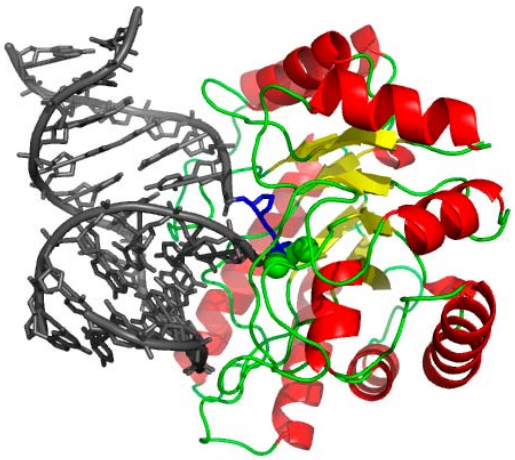

Figure 11. Crystal structure of Endo IV with an abasic site containing DNA.

The flipped abasic site is shown in blue and the three Zn^{2+} ions are colored in green.

process abasic site lesions but also to act on a variety of oxidative damages in DNA (Souza *et al*., 2006). The crystal structure of the *E. coli* Endo IV (Hosfield *et al*., 1999) revealed a TIM barrel fold and the presence of three Zn^{2+} ions buried in a deep, crescent-shaped protein groove. The presence of the metal cofactors and the close position of the C- and the N- termini classify Endo IV in the TIM barrel fold family of "divalent metal dependent enzymes". The high resolution (1.5 Å) crystal structure of Endo IV with its AP-DNA complex (Figure 11) shows severe bending of the DNA backbone of approximately 90°, which promotes double nucleotide flipping and positioning of the extrahelical AP site in an active site pocket, which houses the cluster of three Zn^{2+} ions. This pocket has been proposed to be the main reason for the Endo IV selectivity for abasic sites, since it sterically excludes normal nucleotides (Hosfield *et al*., 1999).

In the suggested mechanisms for the abasic site cleavage, the DNA backbone is incised with the help of the trinuclear zinc cluster, with all three Zn^{2+} ions participating in the catalysis (Figure 12). The role of Zn1 was seen in the crystal structure to be predominantly in activating a water molecule and stabilising the important nucleophile (OH^-), needed for the nucleophilic attack on the target P-O DNA bond. Zn2 together with Glu261 also assists in orienting and activating the attacking nucleophile. The role of Zn3 is mainly in neutralizing the charge of the phosphate group, rendering the phosphorus atom susceptible to nucleophilic substitution. Upon nucleophile attack by the bridging hydroxide, the reaction proceeds trough an intermediate pentacoordinate transition state (Figure 12). All Zn^{2+} ions participate in the stabilisation of the intermediate step. When the transition state collapses to the reaction products, the negative charge at O3' is neutralised by the interaction with Zn3, while Zn2 and Zn1 assist in the stabilisation of the leaving (abasic site containing) group.

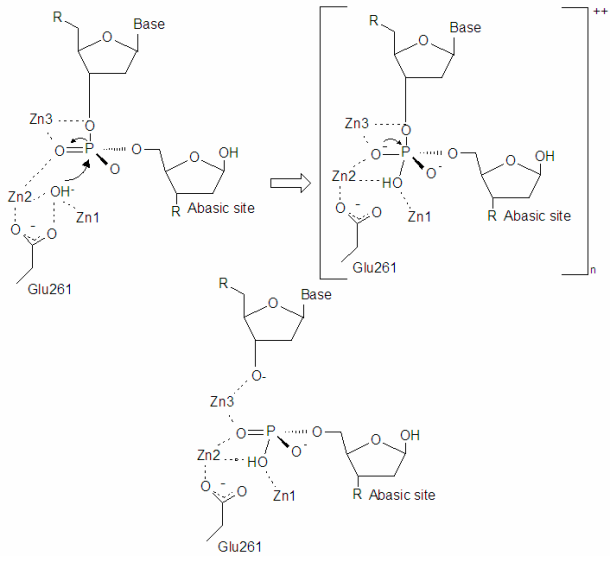

Figure 12. Structure based catalytic mechanism of Endo IV.

Another member of the endonuclease IV family is the *S. cerevisiae* homologue Apn1. Apn1 shows 41 % sequence identity to the *E. coli* Endo IV and also uses three Zn^{2+} for its function.

APE1

In humans, the majority of the 5'AP endonuclease activity is provided by APE1 (Demple *et al*., 1991), also known as HAP1, REF1 and APEX. Unlike Endo IV, APE1 is an Mg^{2+} dependent nuclease.

Crystal structures of the human APE1 bound to a synthetic abasic site-containing DNA, both with and without the divalent Mg^{2+} ion, show how APE1 recognises abasic sites and cleaves the target bond (Beernink *et al*., 2001). In the co-crystal structures, APE1 was seen to flip the abasic nucleotide in an active site protein pocket. The enzyme-DNA interface was seen to include both DNA strands, although the interaction with the AP-DNA strand is pronominal (Figure 13).

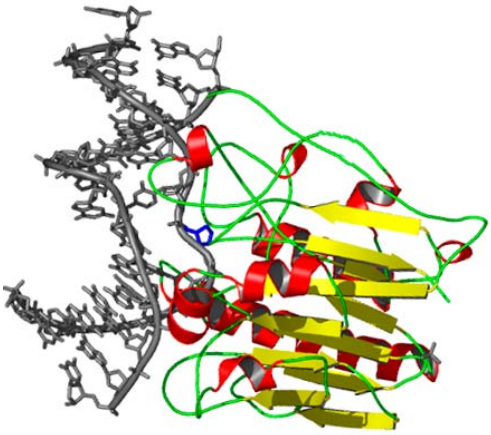

Figure 13. Structure of APE1. The flipped AP site is shown in blue.

Within the pocket the AP-DNA substrate is oriented with the help of one divalent metal ion (Mg^{2+}) and APE1 active-site residues, while Asp210 is aligned for activating the nucleophilic hydroxyl (Figure 14). Upon the nucleophile attack, an intermediate complex is formed and stabilised by Asn212, Asn174, His309 and the single Mg^{2+}. Subsequently, the collapse of the transition state leads to the cleavage of the scissile P-O3' bond, with the O3' leaving group stabilised by the metal ion (Figure 14).

To summarise, in the catalytic reaction of APE1 only one divalent metal cofactor (Mg^{2+}) is used, and unlike endonuclease IV, the magnesium ion is not directly involved in the activation of the catalytic water. This role is performed by Asp210, while the role of the metal cofactor is mainly in the orientation of the target P-O bond, stabilisation of the pentacoordinate intermediate and the O3' leaving group.

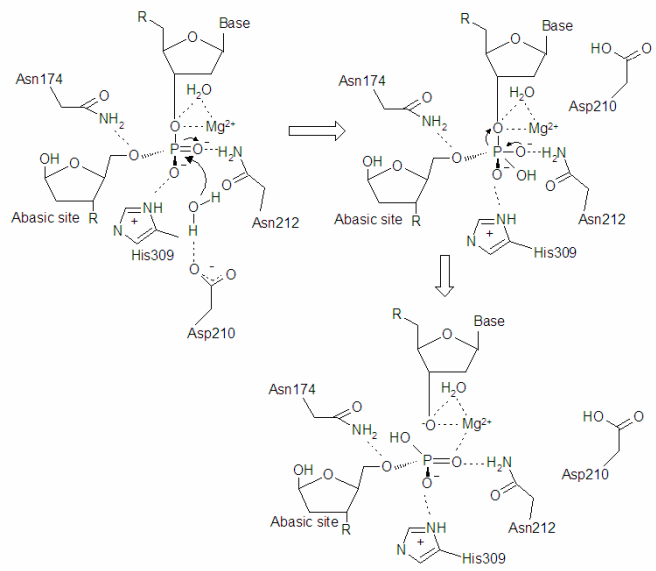

Figure 14. Structure based reaction mechanism for the phosphodiester bond cleavage of APE1.

5. NUCLEOTIDE EXCISION REPAIR

Nucleotide excision repair (NER) is an important mechanism for the removal of a large variety of structurally unrelated DNA lesions such as intra-strand crosslinks (like cisplatin adducts), bulky mono-adducts (like N-2-acetylaminofluorence) and UV induced photoproducts (Van Houten *et al*., 2005). The basic mechanism of NER is conserved in pro- and eukaryotes, but the proteins involved are different. NER can be divided into several steps: damage recognition, dual incision on both sides of the lesion, removal of the damaged oligonucleotide and finally gap filling and sealing of the resulting nick.

Since the most crystal structures are available for the bacterial NER proteins, here only this NER system will be discussed.

5.1 Bacterial NER

The process of NER is performed in *E. coli* by the UvrABC system, which consists of four Uvr proteins: UvrA, UvrB, UvrC, and DNA helicase II (also known as UvrD) (Truglio *et al*., 2006). The UvrA and UvrB enzymes associate in solution, forming an $UvrA_2$-$UvrB_2$ complex (Malta *et al*., 2007). Upon encountering DNA damage, the UvrA dimer is released, while the UvrB dimer remains bound to the DNA (Orren and Sancar, 1990). The process of damage recognition, the UvrA dissociation and the formation of the pre-incision complex are dependent on ATP binding and hydrolysis (Goosen and Moolenaar, 2001). Subsequently, UvrC binds to the $UvrB_2$-DNA preincision complex, displacing one of the UvrB units. UvrC introduces two nicks: first 4

nucleotides from the 3' side of the DNA damage and then 8 nucleotides from the 5' side (Truglio *et al*., 2005), (Verhoeven *et al*., 2000). Subsequently, the DNA fragment containing the damage is removed by the help of UvrD, which also removes the UvrC protein. The resulting gap is then filled in using DNA polymerase I and sealed by DNA ligase.

UvrA

UvrA plays an important role in the *E. coli* NER system initiating the damage recognition and is capable of binding to damaged DNA, even in the absence of the other NER proteins (Truglio *et al*., 2006). At physiological concentrations UvrA is a dimer and its dimerisation, as well as its interactions with DNA, is promoted by ATP binding (Mazur and Grossman, 1991). *E. coli* UvrA has two ATPase domains, both belonging to the ABC (ATP-binding cassette) family of ATPases (Myles and Sancar, 1991), (Gorbalenya, 1990). Each of the ABC ATPase domains consists of a Walker A, a Walker B and an ABC signature motif (Myles and Sancar, 1991).

Recently, a 3.2 Å UvrA crystal structure from *Bacillus stearothermophilus* has been reported (Pakotiprapha *et al*., 2008) (Figure 15). It revealed an UvrA dimer, with each monomer containing six domains: ATP binding domains I and II, signature domains I and II (with the sequence LSGGQ), the UvrB-binding domain and an insertion domain. The ATP-binding domain I and the signature domain I are located in the N-terminal half, while the C-terminal part contains the ATP-binding domain II and the signature domain II. ATP binds to both the ATP binding domain in the N-terminus and to the signature motif in the C-terminus. The main difference

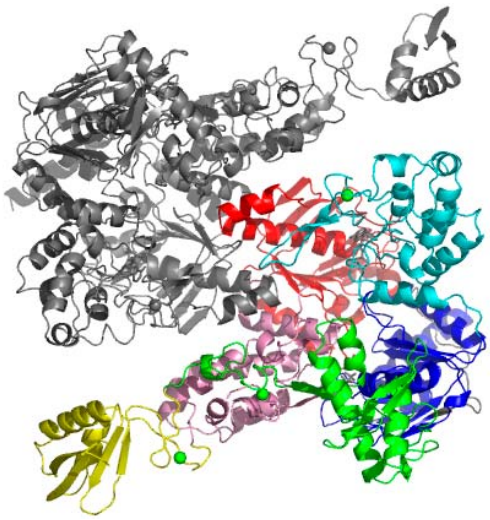

Figure 15. 3.2 Å structure of UvrA from *Bacillus stearothermophilus*.

The UvrB binding domain is in yellow. The signature motif I is shown in pink and the signature motif II in light blue. The ATP binding site I is colored red and the ATP binding site II is represented in dark blue. The insertion domain is colored in green. The Zn atoms are shown as green balls.

between the N- and the C-terminal part of UvrA is the presence of the UvrB binding domain (residues 118 – 256) and the insertion domain (residues 287 – 398) in the N-terminal half, which both contains Zn modules. Deletion mutations in the UvrB binding domain revealed that residues 113 – 245 are crucial for the UvrB-UvrA interactions and based on the UvrB structure it was proposed that they make a contact with domain 2 of UvrB (Pakotiprapha *et al*., 2009).

Anomalous diffraction data obtained from the UvrA structure showed the presence of three Zn atoms. Zn1 is located between the signature domain I and the UvrB binding domain. Zn2 is situated between the signature domain I and the so called insertion domain. Zn3 connects the signature domain II to the dimer interface. The Zn modules do not show a classical Zn finger structure and are proposed to play a structural role (Pakotiprapha *et al*., 2007).

Although the published *B. stearothermophilus* UvrA structure does not contain DNA, based on the sequence conservation and the positive charge Pakotiprapha *et al*. suggested the potential DNA interacting region to be located in the concave side of the UvrA dimer. Unfortunately, the process of UvrA damage recognition is not yet clarified, although it has been suggested that Lys680 and Arg691 might be important for DNA binding, since replacement of these side chains with alanine decrease the UvrA-DNA binding 3 - 37 folds (Croteau *et al*., 2008).

UvrB

UvrB is a central component of the bacterial NER system participating in the important step of damage recognition (Hsu *et al*., 1995). *E. coli* UvrB consists of 673 amino acids and has a molecular weight of 76 kDa. So far three crystal structures of the UvrB protein are available – two from the thermophile organism *Thermus thermophilus* (Machius *et al*., 1999), (Nakagawa *et al*., 1999) and one from a different thermophile *Bacillus caldotenax* (Theis *et al*., 1999) (Figure 16). The three UvrB structures share a similar overall architecture. UvrB consists of five domains: 1a,

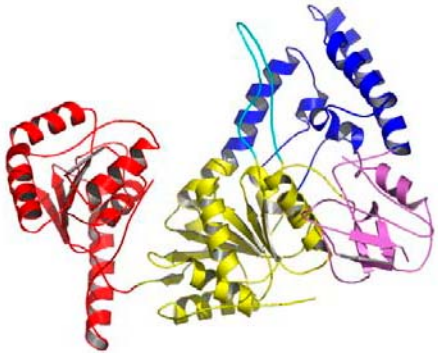

Figure 16. Crystal structure of the DNA Repair enzyme UvrB from *B. caldotenax*.

The hairpin is represented in a light blue color, domain 1a is in yellow, domain 1b is in blue, domain 2 is in pink and domain 3 in red.

1b, 2, 3, 4 (Figure 16). Domain 4 is missing in the crystal structure of *B. caldotenax*, because it is disordered. UvrB domain 4 has been shown to be important for the UvrC binding (Moolenaar *et al*., 1995) and dimerization (Malta *et al*., 2007). An UvrB C-terminal truncation (UvrB*), lacking domain 4, was shown to form a less stable dimer (Verhoeven *et al*., 2002). X-ray (Sohi *et al*., 2000) and NMR structures (Alexandrovich *et al*., 1999) of this UvrB domain are available, and both models agree with it forming a dimer in solution.

An interesting feature of the UvrB structure is the presence of a β-hairpin, situated between domains 1a and 1b (Skorvaga *et al*., 2002). Mutational analysis of the *E. coli* hairpin has shown that aromatic residues (Tyr92 and Tyr93), situated at its bottom, are involved in preventing binding to undamaged DNA (Moolenaar *et al*., 2001).

The importance of the β-hairpin for the DNA binding was confirmed in the recently published structures of UvrB in a complex with DNA having a 3' overhang (Truglio *et al*., 2006). The crystal structure of *B. caldotenax* UvrB bound to this DNA substrate revealed its structure to be highly similar to the native enzyme, the main difference being in the β-hairpin conformation. In the co-crystal of *B. caldotenax* UvrB one of the DNA strands was seen to pass behind the β-hairpin (Truglio *et al*., 2006) and one base from this strand to be flipped out and accommodated into a small hydrophobic pocket. This pocket is too small to accommodate big DNA distortions (for example a cholesterol lesion) and only a planar molecule can fit in. In that aspect, the flipped nucleotide is unlikely to represent the damaged one. A drawback of this crystallized complex is that UvrB it is not bound to a specific DNA damage, but is in a complex with double strand-single strand DNA junction. In that regard, it is difficult to state if the DNA strand observed behind the hairpin represents the damaged- or the non-damaged strand.

Nucleotide flipping by UvrB was demonstrated by using the fluorescent base analogue 2-aminopurine (Malta *et al*., 2006). It was shown that the base at the 3' side of the lesion is inserted into a protein pocket. Furthermore, by using menthol modification covalently attached to a 2-amino purine residue, Malta *et al*. (2008) outlined that the damaged base itself does not change position upon UvrB binding and keeps its intra-helical conformation. Although the exact location of the menthol was not clarified, based on its hydrophobic nature the authors predicted that it also remains buried inside the DNA helix. A model was proposed in which the damaged strand passes behind the β-hairpin and the presence of a damage prevents the translocation of this strand behind the hairpin, which limits the base flipping to the nucleotide 3' to the damage.

UvrC

UvrC is a 68 kDa nuclease, which mediates both the 3' and the 5' incision reactions on damaged DNA upon binding to the UvrB-DNA pre-incision complex (Sancar and Rupp, 1983). Site-directed mutagenesis showed that the 3' incision active site is located in the N-terminal half of the protein (Verhoeven *et al*., 2000), while the site, which carries out the 5' cut is situated in the C-terminal half (Lin and Sancar, 1992). The 3' incision occurs prior to the 5' one (Truglio *et al*., 2005).

Multiple sequence analysis of the N-terminal UvrC part revealed that the catalytic domain is a member of the GIY-YIG family of homing endonucleases (Kowalski *et al*., 1999). The crystal structures of the N-terminal 3' catalytic domains from *B. caldotenax* and *Thermotoga maritima* (Figure 17) have been solved (Truglio *et al*., 2005).

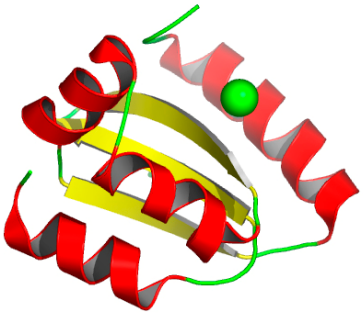

Figure 17. Structure of the C-terminal part of UvrC from *T. maritima*.

The bound metal is shown as green sphere.

Despite soaking and co-crystallization attempts, no divalent metal was detected in the *B. caldotenax* UvrC structure (Truglio *et al*., 2005). The *T. maritima* UvrC did reveal one divalent metal, coordinated by Glu76 and five water molecules, however due to its low occupancy the exact nature of the cofactor was not elucidated. Soaking experiments performed in the presence of $MnCl_2$ suggested that Mn^{2+} can bind within that site, although the fact that Mg^{2+} also stimulates

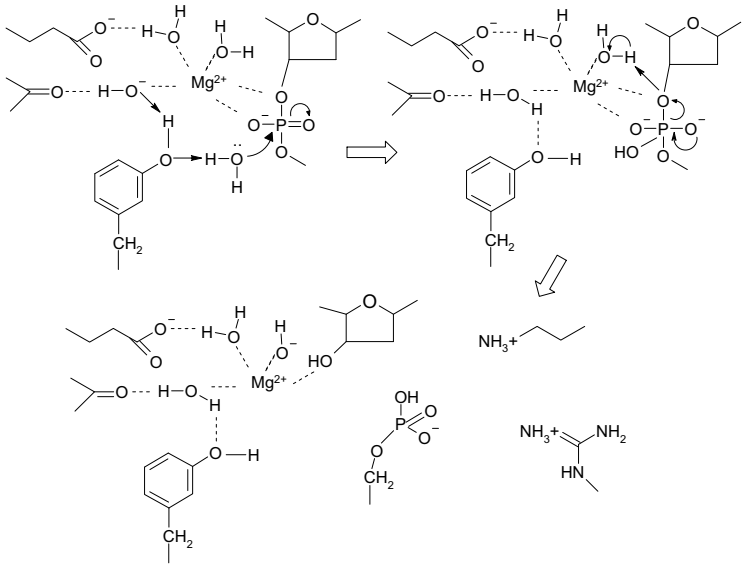

Figure 18. Proposed mechanism for UvrC catalysis.

UvrC activity suggests that the cofactor can also be Mg^{2+}. Although Glu76 was seen as the only protein residue bound directly to the metal, the water molecules coordinating the metal formed additional contacts with the protein side chains. Mutation of Glu76 proved the crucial role of this residue for the UvrC function, since the alanine substitution resulted in a catalytically inactive UvrC enzyme (Truglio *et al*., 2005).

Interestingly, from the structural data the molecule acting as the general acid in the catalytic process was not found and it was proposed that one of the metal coordinated water molecules performs this function (Truglio *et al*., 2005). Furthermore, Tyr29, which is situated in close proximity to the divalent cation (4.3 Å), was suggested to act as the general base by accepting a proton from the nucleophilic water molecule and simultaneously transferring its proton to the metal-bound hydroxide (Figure 18).

The C-terminal 219 amino acids of the UvrC from *T. maritima* were crystallised (Karakas *et al*., 2007) and revealed an endonuclease domain responsible for the 5' incision event (residues 341 – 494), followed by a pair of helix–hairpin–helix (HhH) motifs (residues 497 – 557), that form an $(HhH)_2$ domain implicated in DNA binding (Figure 19). A very short linker (residues 495 and 496) connects the two domains.

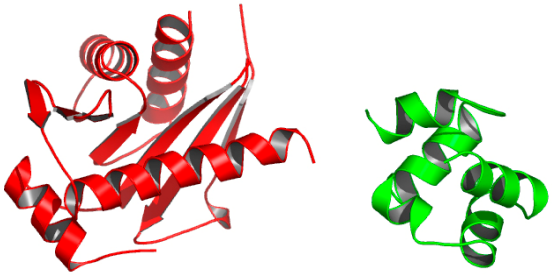

Figure 19. Structure of the C-terminal part of UvrC from *T. maritima*.

The endonuclease and the $(HhH)_2$ domain are shown in red and green, respectively.

The core of the UvrC 5' endonuclease domain has a fold belonging to the Rnase H family of enzymes. Divalent cations (Mg^{2+} or Mn^{2+}) are required by Rnase H-like enzymes to bind to their substrate and catalyze the nucleotidyl transfer reactions (Krakowiak *et al*., 2002). $MnCl_2$ soaking experiments with UvrC revealed one catalytic Mn^{2+}, coordinated by His488. Two catalytic aspartates (Asp367 and Asp429) interact indirectly with the cation through water molecules. Since the H488A mutant is still able to perform the 5' incision, albeit with a reduced rate, it is unlikely that this residue is solely responsible for metal coordination. Based on the similarity of UvrC C-terminal domain to the Rnase H-like enzymes a two metal ions catalysis was proposed for the UvrC 5' incision, where the binding of the second metal depends greatly on the presence of a nucleic acid substrate (Karakas *et al*., 2007).

6. UVDE

6.1 Discovery and initial characterisation of UVDE

Analysis of the radiation sensitivity of the yeast *Schizosaccharomyces pombe* led to the identification of a group of mutants, which phenotype could not be explained by defects in the NER system (Phipps *et al*., 1985). Later it was found that *S. pombe* rad mutants, which are deficient in NER, are only moderately UV sensitive and still capable of efficient removal of both CPD and 6-4PP UV lesions via a light independent pathway (McCready *et al*., 1993), (Sidik *et al*., 1992). Based on these data it was proposed that *S. pombe* possesses a novel excision repair pathway for removal of UV induced lesions (Yonemasu *et al*., 1997). The first biochemical evidence that this pathway exists was the identification of an ATP-independent UV damage-dependent endonuclease in *S. pombe* cell extracts (Bowman *et al*., 1994). The enzyme was initially named *S. pombe* DNA endonuclease (SPDE), but was renamed later to UV damage endonuclease (UVDE). The initial biochemical analysis revealed that UVDE (also designated Uvelp) cleaves the DNA phosphodiester backbone directly 5' to both CPD and 6-4PP lesions (Bowman *et al*., 1994). The isolation of the uve1 gene (Takao *et al*., 1996) and the biochemical characterization of a truncated UVDE protein (Kaur *et al*., 1998) revealed a much broader substrate specificity of the *S. pombe* UVDE than originally suspected.

6.2 Biochemical characterisation of *S. pombe* UVDE

The full length uve1 gene encodes a 599 amino acid protein of approximately 68.8 kDa, which when overexpressed in either *E. coli* or *S. cerevisiae* cells, yields a relatively unstable protein that rapidly loses activity (Kaur *et al*., 1998). In an attempt of obtaining an *S. pombe* UVDE protein with better stability several affinity tagged truncations were purified and their activity towards UV lesions analysed. Most of the truncated proteins contained N-terminal deletions with different length with a sharp decline in activity for truncations longer than 232 amino acids (Takao *et al*., 1996). Truncations of the C-terminal part of UVDE were shown to have more drastic effect, since even a relatively short deletion of 35 residues abrogates activity (Takao *et al*., 1996). Based on these findings, the essential region for the activity of the *S. pombe* UVDE was proposed to include the C-terminal two thirds of the protein. Kaur *et al*. conducted a detailed biochemical characterisation of a highly stable 228 residue N-terminal truncation of UVDE. This protein was shown to have broad substrate specificity and being active in a large range of salt concentrations with a pH optimum between pH 6.0 and 6.5.

6.3 Activity of UVDE on UV induced lesions

The initial studies of *S. pombe* UVDE demonstrated that this enzyme is capable of recognising both *cis-syn* CPDs and 6-4 PPs (Bowman *et al*., 1994). Later, the incision activity of UVDE was determined on a series of UV induced lesions: *cis-syn* CPD (89 % incision), *trans-syn* I CPD (75 %), *trans-syn* II CPD (75 %), 6-4 PP (71 %) and the Dewar 6-4 PP isomer (83 %), (Avery

et al., 1999). Each of the UV photoproducts listed above, causes different distortion when incorporated into DNA, showing the capacity of UVDE to recognise a range of structurally unrelated damages.

6.4 Activity of UVDE on abasic sites

UVDE was shown to cleave DNA substrates containing abasic sites in a manner similar to the AP endonucleases (Tanihigashi *et al*., 2006), introducing a nick directly 5' to the abasic site and producing 3'-hydroxyl and 5'-deoxyribose phosphate (Avery *et al*., 1999). However, unlike the AP endonucleases, UVDE introduces a second nick one nucleotide away from the lesion (Avery *et al*., 1999). The presence of a second nick, however, is highly dependent on the DNA sequence. The UVDE activity on the abasic site as well as its actual incision position will be addressed in further details in Chapter 4 of this thesis. Abasic site substrates containing either A or G opposite to the lesions are processed by *N. crassa* UVDE with equal efficiency, whereas lesions with C or T opposite are cleaved less efficiently (Kano *et al*., 1999), suggesting that UVDE interacts with the undamaged DNA strand. The same authors demonstrated that introduction of UVDE into *E. coli* mutants lacking both of its major AP endonucleases (exonuclease III and endonuclease IV) gave the host cells a resistance to abasic sites introducing agents such as methyl methane sulfonate (MMS) and butylhydroperoxide, however to lesser extent than the AP endonucleases. Based on these findings, a new role has been proposed for UVDE (Kanno *et al.,* 1999) as being part of an alternative repair system for abasic sites. Our findings, however, question this notion, as it will be shown in Chapter 5, that not all UVDE enzymes recognise the abasic site efficiently. Furthermore, the activity of *S. pombe* UVDE on the abasic site is strictly sequence dependent.

6.5 Recognition of base-base mismatches

In vitro studies (Kaur *et al*., 1999) established that to various extents, UVDE also recognises and cleaves single base mismatches. Moreover, it was shown by the same authors that mutants lacking the *uve1* gene display spontaneous mutator phenotype, underlining their hypothesis that UVDE might play a role in mismatch repair (Kunz *et al*., 2001). The sites of UVDE cleavage were mapped to be 5' immediately to the impaired base and/or one nucleotide further away, dependent on the specific mismatch. The cleavage efficiency was also shown to vary significantly (from 5 % to 40 %), depending on the nature of the base mispair (Kaur *et al*., 1999). The low incision efficiency of UVDE questions the role of this enzyme as an alternative pathway for mismatch repair. The observed mutator phenotype of the *uve1* mutants might also be caused by reduced removal of abasic sites.

UVDE has also been shown to incise duplex DNA containing small loops and hairpins, albeit again with a very low efficiency. A study performed by Kaur and Doetsch (Kaur and Doetsch, 2000) demonstrated that UVDE incises DNA containing small loops of 2-4 nucleotides in length. The position of the nick, however, is not as expected directly 5' to the loop but several nucleotides away. Similar behaviour has been observed also on a Pt-crosslink, where the incision

position is also not directly adjacent to the damage. What determines the position of the UVDE cut will be further elucidated in Chapter 4. Larger loops of 6-8 nucleotides in length are not a substrate for UVDE. DNA with palindromic insertions that could form base-paired hairpin structures is also not nicked by UVDE.

6.7 Distribution of UVDE homologues

The distribution of UVDE has been recently reviewed by Goosen and Moolenaar (2007). Homologues of the UVDE protein have been identified in 4 archaebacteria and in 30 eubacterial species, as well as in several fungi. A number of closely related *Bacillus* species (*Bacillus anthracis*, *Bacillus cereus* and *Bacillus thuringiensis*) contain even two UVDE homologues. It has been suggested (Goosen and Moolenaar, 2007) that one of the UVDE gene products is expressed in the vegetative state, while the other is specifically expressed upon spore germination. Another possibility is that the two UVDE enzymes exhibit difference in their substrate specificities, since in spores a specific spore photoproduct is formed upon UV irradiation. The only species outside the *Bacillales* that also contain two copies of UVDE is *Clostridium beyerinckii*, which is also a spore-forming bacterium (Goosen and Moolenaar, 2007). A homologous protein to the *S. pombe* UVDE has been also found in the *Deinococcus radiodurans*. Unlike the Δ*uvrA* strains of *E. coli,* the Δ*uvrA* strains of *D. radiodurans* exhibit nearly wild-type levels of resistance to UV light (Earl *et al*., 2002).

Interestingly, the N-terminal one third of the UVDE protein is not conserved in the eukaryotic homologues and completely absent in the bacterial ones. The N-terminal region is highly hydrophilic, as it includes many charged amino acids. The C-terminal part of the protein varies in length and also contains a number of charged residues. The function of these extensions is as yet unknown.

6.8 The UVDE repair pathway

A simple model has been proposed for the steps following the nicking activity of UVDE (Yasui and McCready, 1998). The repair process was suggested to be completed by simply removing a segment of DNA containing the UV photoproduct with a 5' - 3' exonuclease (or with an endonuclease cutting 3' to the UV photoproduct site), filling the gap by a polymerase and sealing the resulting nick by a DNA ligase (Doetsch 1995). Epistatic analyses have implicated several gene products to be involved in the UVDE-initiated DNA repair, including the *S. pombe* FEN-1 (flap endonuclease) homolog and the exonuclease Rad2p (Yoon *et al*., 1999). The first complete *in vitro* reconstitution of the UVDE pathway has been given by Alleva *et al*. (2000). Two distinct pathways have been proposed. In the first pathway upon the 5' nick introduced by UVDE, the damage is removed by the 5' to 3' exonuclease activity of Rad2p, resulting in formation of a gap. The gap is subsequently filled by polymerase δ in a presence of PCNA (Proliferating Cell Nuclear Antigen) and RFC (Replication Factor C) and the resulting nick sealed by a ligase. Alternatively, the DNA polymerase can first extend the free 3' end produced after the UVDE

nicking activity, thus creating a misplaced 5' flap. This flap structure is a substrate for the FEN-1 flap-endonuclease activity. The resulting nick is again sealed by a ligase.

The broad substrate specificity of UVDE poses the question why bacterial species have both UVDE and the NER repair pathways. Although the substrate specificities of both systems overlap to some extent, NER distinguish itself with broader substrate specificity that UVDE. On the CPD lesion, however, the UVDE is beneficial since it repairs this lesion with high affinity.

REFERENCES

Alexandrovich A, Sanderson MR, Moolenaar GF, Goosen N and Lane AN, NMR assignments and secondary structure of the UvrC binding domain of UvrB, *FEBS Lett*. **451** (1999), pp. 181-185

Alleva JL, Zuo S, Hurwitz J and Doetsch PW, In vitro reconstitution of the *Schizosaccharomyces pombe* alternative excision repair pathway, *Biochemistry* **39** (2000), pp. 2659-2666

Avery AM, Kaur B, Taylor JS, Mello JA, Essigmann JM and Doetsch PW, Substrate specificity of ultraviolet DNA endonuclease (UVDE/Uve1p) from *Schizosaccharomyces pombe*, *Nucleic Acids Res*. **27** (1999), pp. 2256-2264

Beernink T, Segelke W, Hadi Z, Erzberger P, Wilson M 3rd and Rupp B, Two divalent metal ions in the active site of a new crystal form of human apurinic/apyrimidinic endonuclease, Ape1: implications for the catalytic mechanism, *J. Mol. Biol*. **307** (2001), pp. 1023-1034

Bowman KK, Sidik K, Smith CA, Taylor JS, Doetsch PW and Freyer GA, A new ATP-independent DNA endonuclease from *Schizosaccharomyces pombe* that recognizes cyclobutane pyrimidine dimers and 6-4 photoproducts, *Nucleic Acids Res*. **22** (1994), pp. 3026-3032

Carell T, Burgdorf LT, Kundu LM and Cichon M, The mechanism of action of DNA photolyases, *Curr. Opin. Chem. Biol*. **5** (2001), pp. 491-498

Carey F and Sundberg R, Advanced organic chemistry, 3rd edition. Plenium Publishing Corporation, New York (2000)

Croteau DL, DellaVecchia MJ, Perera L and Van Houten B, Cooperative damage recognition by UvrA and UvrB: identification of UvrA residues that mediate DNA binding, *DNA Repair* (*Amst*.) **7** (2008), pp. 392-404

Daniels DS, Woo TT, Luu KX, Noll DM, Clarke ND, Pegg AE and Tainer JA, DNA binding and nucleotide flipping by the human DNA repair protein AGT, *Nat. Struct. Mol. Biol*. **1** (2004), pp. 714-720

David S, Goodsell, the Molecular Perspective: Ultraviolet Light and Pyrimidine Dimers, Oncologist **6** (2001), pp. 298-299

Demple B, Herman T and Chen S, Cloning and expression of APE, the cDNA encoding the major human apurinic endonuclease: definition pf a family of DNA repair enzymes, *Proc. Natl. Acad. Sci. USA*. **88** (1991), pp. 11450-11454

Demple B and Linn S, 5,6-saturated thymine lesions in DNA: production by ultraviolet light or hydrogen peroxide, *Nucleic Acids Res*. **10** (1982), pp. 3781-3789

Demple B, Sedgwick B, Robins P, Totty N, Waterfield MD and Lindahl T, Active site and complete sequence of the suicidal methyltransferase that counters alkylation mutagenesis, *Proc. Natl. Acad. Sci. USA*. **82** (1985), pp. 2688-2692

Doetsch PW, What's old is new: an alternative DNA excision repair pathway, *Trends Biochem. Sci.* **20** (1995), pp. 384-386

Drohat AC, Jagadeesh J, Ferguson E and Stivers JT, Role of electrophilic and general base catalysis in the mechanism of *Escherichia coli* uracil DNA glycosylase, *Biochemistry* **8** (1999), pp. 11866-11875

Earl AM, Rankin SK, Kim KP, Lamendola ON and Battista JR, Genetic evidence that the uvsE gene product of *Deinococcus radiodurans R1* is a UV damage endonuclease, *J. Bacteriol*. **184** (2002), pp. 1003-1009

Essen LO and Klar T, Light-driven DNA repair by photolyases, *Cell. Mol. Life Sci*. **63** (2006), pp. 1266-1277

Etzkorn C and Horton C, Ca^{2+} binding in the active site of *Hinc*II: implications for the catalytic mechanism, *Biochemistry* **43** (2004), pp. 13256-13270

Fersht A, Structure and Mechanism in Protein Science: a guide to enzyme catalysis and protein folding, W. H. Freeman and Co., New York (1999)

Friedberg C and King J, Dark repair of ultraviolet-irradiated deoxyribonucleic acid by bacteriophage T4: purification and characterization of a dimer-specific phage-induced endonuclease, *J. Bacteriol*. **106** (1971), pp. 500-507

Friedberg C, Walker C, Siede W, Wood D, Schultz A and Ellenberger T, DNA Repair and Mutagenesis, 2nd Edition, ASM Press (2005)

Galburt E and Stoddard B, Catalytic mechanisms of restriction and homing endonucleases, *Biochemistry* **41** (2002), pp. 13851-13860

Gerlt J, Mechanistic principles of enzyme-catalysed cleavage of phosphodiester bonds, Nucleases, 2nd edition, Cold Spring Harbor Laboratory Press (1993)

Gerlt J, Phosphate ester hydrolysis, *Enzymes* **20** (1992), pp. 95-139

Golan G, Zharkov O, Grollman P, Dodson L, McCullough K, Lloyd S and Shoham G, Structure of T4 pyrimidine dimer glycosylase in a reduced imine covalent complex with abasic site-containing DNA, *J. Mol. Biol*. **362** (2006), pp. 241-258

Goodtzova K, Kanugula S, Edara S, Pauly GT, Moschel RC and Pegg AE, Repair of O6-benzylguanine by the *Escherichia coli* Ada and Ogt and the human O6-alkylguanine-DNA alkyltransferases, *J. Biol. Chem*. **272** (1997), pp. 8332-8338

Goosen N and Moolenaar GF, Repair of UV damage in bacteria, *DNA Repair* (*Amst*.) **7** (2007), pp. 353-379

Goosen N and Moolenaar GF, Role of ATP hydrolysis by UvrA and UvrB during NER, *Res. Microbiol*. **152** (2001), pp. 401-409

Gorbalenya AE and Koonin EV, Superfamily of UvrA-related NTP-binding proteins. Implications for rational classification of recombination/repair systems, *J. Mol. Biol*. **213** (1990), pp. 583-591

Guo H, Yang H, Mockler TC and Lin C, Regulation of flowering time by *Arabidopsis* photoreceptors, *Science* **279** (1998), pp. 1360-1363

Guthrie J, Hydration and dehydration of phosphoric acid derivatives: Free energies of formation of the pentacoordinate intermediates for phosphate ester hydrolysis and of monomeric monophosphate, *J. Chem. Soc*. **99** (1997), pp. 3391-4001

Hitomi K, Nakamura H, Kim S.-T, Mizukoshi T, Ishikawa T, Iwai S and Todo T, Role of two histidines in the (6–4) photolyase reaction, *J. Biol. Chem*. **276** (2001), pp. 10103-10109

Hori N, Doi T, Karaki Y, Kikuchi M, Ikenhara M and Ohtsuka E, Participation of glutamic acid 23 of T4 endonuclease V in the beta-elimination reaction of an abasic site in synthetic duplex DNA, *Nucleic Acid Res*. **20** (1993), pp. 4761-4764

Horton JR and Cheng X, *Pvu*II endonuclease contains two calcium ions in active sites, *J. Mol. Biol*. **300** (2000), pp. 1049-1056

Hosfield J, Guan Y, Haas J, Cunningham P and Tainer A, Structure of the DNA repair enzyme endonuclease IV and its DNA complex: double-nucleotide flipping at abasic sites and three-metal-ion catalysis, *Cell* **98** (1999), pp. 397-408

Hsu DS, Kim ST, Sun Q and Sancar A, Structure and function of the UvrB protein, *J. Biol. Chem*. **270** (1995), pp. 8319-8327

Husain I, Griffith J and Sancar A, Thymine dimers bend DNA, *Proc. Natl. Acad. Sci. USA*. **85** (1988), pp. 2558-2562

Jackson PE, Hall CN, O'Connor PJ, Cooper DP, Margison GP and Povey AC, Low O6-alkylguanine DNA-alkyltransferase activity in normal colorectal tissue is associated with colorectal tumours containing a GC→AT transition in the K-ras oncogene, *Carcinogenesis* **18** (1997), pp. 1299-1302

Jencks W, How does a reaction choose its mechanism? *Chem. Soc. Rev.* **10** (1981), pp. 345-375

Jing Y, Kao JF and Taylor JS, Thermodynamic and base-pairing studies of matched and mismatched DNA dodecamer duplexes containing *cis-syn*, (6-4) and Dewar photoproducts of TT, *Nucleic Acids Res*. **26** (1998), pp. 3845-3853

Kanno S, Iwai S, Takao M and Yasui A, Repair of apurinic/apyrimidinic sites by UV damage endonuclease; a repair protein for UV and oxidative damage, *Nucleic Acids Res*. **27** (1999), pp. 3096-3103

Kanugula S, Goodtzova K and Pegg AE, Probing of conformational changes in human O^6-alkylguanine-DNA alkyl transferase protein in its alkylated and DNA-bound states by limited proteolysis, *Biochem J*. **32** (1998), pp. 545-545

Karakas E, Truglio JJ, Croteau D, Rhau B, Wang L, Van Houten B and Kisker C, Structure of the C-terminal half of UvrC reveals an RNase H endonuclease domain with an Argonaute-like catalytic triad, *EMBO J*. **26** (2007), pp. 613-622

Kaur B, Avery AM and Doetsch PW, Expression, purification, and characterization of ultraviolet DNA endonuclease from *Schizosaccharomyces pombe*, *Biochemistry* **37** (1998), pp. 11599-11604

Kaur B and Doetsch PW, Ultraviolet damage endonuclease (Uve1p): a structure and strand-specific DNA endonuclease, *Biochemistry* **39** (2000), pp. 5788-5796

Kaur B, Fraser JL, Freyer GA, Davey S and Doetsch PW, A Uve1p-mediated mismatch repair pathway in *Schizosaccharomyces pombe*, *Mol. Cell. Biol*. **19** (1999), pp. 4703-4710

Kavli B, Sundheim O, Akbari M, Otterlei M, Nilsen H, Skorpen F, Aas PA, Hagen L, Krokan HE and Slupphaug G, hUNG2 is the major repair enzyme for removal of uracil from U:A matches, U:G mismatches, and U in single-stranded DNA, with hSMUG1 as a broad specificity backup, *J. Biol. Chem*. **277** (2002), pp. 39926-39936

Kim JK and Choi BS, The solution structure of DNA duplex-decamer containing the (6-4) photoproduct of thymidylyl (3'→5') thymidine by NMR and relaxation matrix refinement, *Eur. J. Biochem*. **228** (1995), pp. 849-854

Kim ST, Heelis PF, Okamura T, Hirata Y, Mataga N and Sancar A, Determination of rates and yields of interchromophore (folate→flavin) energy transfer and intermolecular (flavin→DNA) electron transfer in *Escherichia coli* photolyase by time-resolved fluorescence and absorption spectroscopy, *Biochemistry* **30** (2001), pp. 11262-11270

Kim ST, Heelis PF and Sancar A, Energy transfer (deazaflavin→FADH2) and electron transfer (FADH2→TT) kinetics in *Anacystis nidulans* photolyase, *Biochemistry* **31** (1992), pp. 11244-11248

Kobayashi K, Kanno S, Smit B, van der Horst GT, Takao M and Yasui A, Characterization of photolyase/blue-light receptor homologs in mouse and human cells, *Nucleic Acids Res*. **26** (1998), pp. 5086-5092

Kobayashi Y, Ishikawa T, Hirayama J, Daiyasu H, Kanai S, Toh H, Fukuda I, Tsujimura T, Terada N, Kamei Y, Yuba S, Iwai S and Todo T, Molecular analysis of zebrafish photolyase/cryptochrome family: two types of cryptochromes present in zebrafish, *Genes Cells* **5** (2000), pp. 725-738

Kowalski JC, Belfort M, Stapleton MA, Holpert M, Dansereau JT, Pietrokovski S, Baxter SM and Derbyshire V, Configuration of the catalytic GIY-YIG domain of intron endonuclease I-TevI: coincidence of computational and molecular findings, *Nucleic Acids Res*. **27** (1999), pp. 2115-2125

Krakowiak A, Owczarek A, Kozio□kiewicz M and Stec WJ, Stereochemical course of *Escherichia coli* RNase H, *Chembiochem*. **3** (2002), pp. 1242-1250

Kunz C and Fleck O, Role of the DNA repair nucleases Rad13, Rad2 and Uve1 of *Schizosaccharomyces pombe* in mismatch correction, *J. Mol. Biol*. **313** (2001), pp. 241-253

Lee JH, Hwang GS, Kim JK and Choi BS, The solution structure of DNA decamer duplex containing the Dewar product of thymidylyl (3→5') thymidine by NMR and full relaxation matrix refinement, *FEBS Lett*. **428** (1998), pp. 269-274

Lin JJ and Sancar A, Active site of (A)BC excinuclease I. Evidence for 5' incision by UvrC through a catalytic site involving Asp399, Asp438, Asp466, and His538 residues, *J. Biol. Chem*. **267** (1992), pp. 17688-17692

Lindahl T and Nyberg B, Heat-induced deamination of cytosine residues in deoxyribonucleic acid, *Biochemistry* **13** (1974), pp. 3405-3410

Lindahl T, An N-glycosidase from *Escherichia coli* that releases free uracil from DNA containing deaminated cytosine residues, *Proc. Natl. Acad. Sci. USA*. **71** (1974), pp. 3649-3653

Liu H, Hewitt SR and Hays JB, Antagonism of ultraviolet-light mutagenesis by the methyl-directed mismatch-repair system of *Escherichia coli*, *Genetics* **154** (2000), pp. 503-512

Ljungquist S, A new endonuclease from *Escherichia coli* acting at apurinic sites in DNA, *J. Biol Chem*. **252** (1977), pp. 2808-2814

Machius M, Henry L, Palnitkar M and Deisenhofer J, Crystal structure of the DNA nucleotide excision repair enzyme UvrB from *Thermus thermophilus*, *Proc. Natl. Acad. Sci. USA*. **96** (1999), pp. 11717-11722

Malta E, Moolenaar GF and Goosen N, Base flipping in nucleotide excision repair, *J. Biol. Chem*. **281** (2006), pp. 2184-2194

Malta E, Moolenaar GF and Goosen N, Dynamics of the UvrABC nucleotide excision repair proteins analyzed by fluorescence resonance energy transfer, *Biochemistry* **46** (2007), pp. 9080-9088

Malta E, Verhagen CP, Moolenaar GF, Filippov DV, van der Marel GA and Goosen N, Functions of base flipping in *E. coli* nucleotide excision repair, *DNA Repair* (*Amst*.) **7** (2008), pp. 1647-1658

Mazur SJ and Grossman L, Dimerisation of *E. coli* UvrA and its binding to undamaged and ultraviolet light damaged DNA, *Biochemistry* **30** (1991), pp. 4431-4443

McClarin A, Frederick C, Wang C, Greene P, Boyer W, Grable J and Rosenberg M, Structure of the DNA-*Eco*RI endonucleases recognition complex at 3 Å resolution, *Science* **234** (1986), pp. 1526-1534

McCready S, Carr AM and Lehmann AR, Repair of cyclobutane pyrimidine dimers and 6-4 photoproducts in the fission yeast *Schizosaccharomyces pombe*, *Mol. Microbiol*. **10** (1993), pp. 885-890

Mees A, Klar T, Gnau P, Hennecke U, Eker AP, Carell T and Essen LO, Crystal structure of a photolyase bound to a CPD-like DNA lesion after in situ repair, *Science* **306** (2004), pp. 1789-1793

Minton K, Durphy M, Taylor R and Friedberg C. The ultraviolet endonuclease of bacteriophage T4: further characterization. *J. Biol. Chem*. **250** (1975), pp. 2823-2829

Mitchell DL, Jen J and Cleaver JE, Sequence specificity of cyclobutane pyrimidine dimers in DNA treated with solar (ultraviolet B) radiation, *Nucleic Acids Res*. **20** (1992), pp. 225-229

Mitchell DL and Nairn RS, The biology of the (6-4) photoproduct, *Photochem. Photobiol*. **49** (1989), pp. 805-819

Moolenaar GF, Franken KL, Dijkstra DM, Thomas-Oates JE, Visse R, van de Putte P and Goosen N, The C-terminal region of the UvrB protein of *Escherichia coli* contains an important determinant for UvrC binding to the preincision complex but not the catalytic site for 3'-incision, *J. Biol. Chem*. **270** (1995), pp. 30508-30515

Moolenaar GF, Höglund L and Goosen N, Clue to damage recognition by UvrB: residues in the beta-hairpin structure prevent binding to non-damaged DNA, *EMBO J.* **20** (2001), pp. 6140-6149

Moore MH, Gulbis JM, Dodson EJ, Demple B and Moody PCE, Crystal structure of a suicidal DNA repair protein: the Ada O^6-methylguanine-DNA methyltransferase from *E. coli*, *EMBO J.* **13** (1994), pp. 1495-1501

Morikawa K, Matsumoto O, Tsujimoto M, Katayanagi K, Ariyoshi M, Doi T, Ikehara M, Inaoka T and Ohtsuka E, X-ray structure of T4 endonuclease V: an excision repair enzyme specific for a pyrimidine dimmer, *Science* **256** (1992), pp. 523-526

Myles GM and Sancar A, Isolation and characterization of functional domains of UvrA, *Biochemistry* **30** (1991), pp. 3834-3840

Nakabeppu Y, Yamashita K and Sekiguchi M, Purification and characterization of normal and mutant forms of T4 endonuclease V, *J. Biol. Chem.* **257** (1982), pp. 2556-2562

Nakagawa N, Sugahara M, Masui R, Kato F, Fukuyama K and Kuramitsu S, Crystal structure of *Thermus thermophilus* HB8 UvrB protein, a key enzyme of nucleotide excision repair, *J. Biochem.* **126** (1999), pp. 986-990

Nakajima S, Sugiyama M, Iwai S, Hitomi K, Otoshi E, Kim S.-T, Jiang C.-Z, Todo T, Britt AB and Yamamoto K, Cloning and characterization of a gene (*UVR3*) required for photorepair of 6-4 photoproducts in *Arabidopsis thaliana*, *Nucleic Acids Res.* **26** (1998), pp. 638-644

Newman M, Lunnen K, Wilson G, Greci J, Schildkraut I and Phillips SE, Crystal structure of restriction endonuclease *Bgl*I bound to its interrupted DNA recognition sequence, *EMBO J.* **17** (1998), pp. 5466-5476

Orren DK and Sancar A, Formation and enzymatic properties of the UvrB-DNA complex, *J. Biol. Chem.* **265** (1990), pp. 15796-15803

Paalman SR, Sung C and Clarke ND, Specificity of DNA repair methyltransferases determined by competitive inactivation with oligonucleotide substrates: evidence that *Escherichia coli* Ada repairs O^6-methylguanine and O^4-methylthymine with similar efficiency, *Biochemistry* **37** (1997), pp. 11118-11124

Pakotiprapha D, Inuzuka Y, Bowman BR, Moolenaar GF, Goosen N, Jeruzalmi D and Verdine GL, Crystal structure of *Bacillus stearothermophilus* UvrA provides insight into ATP-Modulated dimerization, UvrB interaction, and DNA binding, **29** *Mol. Cell* (2008), pp. 122-133

Parikh SS, Walcher G, Jones GD, Slupphaug G, Krokan HE, Blackburn GM and Tainer JA, Uracil-DNA glycosylase-DNA substrate and product structures: conformational strain promotes catalytic efficiency by coupled stereoelectronic effects, *Proc. Natl. Acad. Sci. USA.* **97** (2000), pp. 5083-5088

Park H, Zhang K, Ren Y, Nadji S, Sinha N, Taylor JS and Kang C, Crystal structure of a DNA decamer containing a *cis-syn* thymine dimer, *Proc. Natl. Acad. Sci. USA.* **99** (2000), pp. 5965-5970

Paspaleva K, Thomassen E, Pannu NS, Iwai S, Moolenaar GF, Goosen N and Abrahams JP, Crystal structure of the DNA repair enzyme ultraviolet damage endonuclease, *Structure* **15** (2007), pp. 1316-1324

Pearl L, Structure and function in the uracil-DNA glycosylase superfamily, *Mutat. Res.* **460** (2000), pp. 165-181

Pearlman DA, Holbrook SR, Pirkle DH and Kim SH, Molecular models for DNA damaged by photoreaction, *Science* **227** (1985), pp. 1304-1308

Phipps J, Nasim A and Miller DR, Recovery, repair, and mutagenesis in *Schizosaccharomyces pombe*, *Adv. Genet.* **23** (1985), pp. 1-72

Pingoud A, Fuxreiter M, Pingoud V and Wende W, Type II restriction endonucleases: structure and mechanism, *Cellular and Molecular Life Sciences* (*CMLS*) **62** (2005), pp. 685-707

Samson L, The suicidal DNA repair methyltransferases of microbes, *Mol. Microbiol.* **6** (1992), pp. 825-831

Sancar A and Rupp WD, A novel repair enzyme: UVRABC excision nuclease of *Escherichia coli* cuts a DNA strand on both sides of the damaged region, *Cell* **33** (1983), pp. 249-260

Sancar GB, Enzymatic photoreactivation: 50 years and counting, *Mutat. Res.* **451** (2000), pp. 25-37

Sedgwick B, Bates PA, Paik J, Jacobs SC and Lindahl T, Repair of alkylated DNA, *DNA Repair* (*Amst.*) **6** (2007), pp. 429-442

Sidik K, Lieberman HB and Freyer GA, Repair of DNA damaged by UV light and ionizing radiation by cell-free extracts prepared from *Schizosaccharomyces pombe*, *Proc. Natl. Acad. Sci. USA*. **89** (1992), pp. 1212-1216

Skorvaga M, Theis K, Mandavilli BS, Kisker C and Van Houten B, The β-hairpin motif of UvrB is essential for DNA binding, damage processing and UvrC-mediated incisions, *J. Biol. Chem*. **277** (2002), pp. 1553-1559

Smith A and Taylor S, Preparation and characterization of a set of deoxyoligonucleotide 49-mers containing site-specific *cis-syn*, *trans-syn*-I, (6-4) and Dewar photoproducts of thymidylyl (3'-5') thymidine, *Biol. Chem*. **268** (1993), pp. 11143-11151

Sohi M, Alexandrovich A, Moolenaar G, Visse R, Goosen N, Vernede X, Fontecilla-Camps JC, Champness J and Sanderson MR, Crystal structure of *Escherichia coli* UvrB C-terminal domain, and a model for UvrB-uvrC interaction, *FEBS Lett*. **465** (2000), pp. 161-164

Souza L, Eduardo R, Padula M and Leitao C, Endonuclease IV and exonuclease III are involved in the repair and mutagenesis of DNA lesions induced by UVB in *Escherichia coli*, *Mutagenesis* **21** (2006), pp. 125-130

Takao M, Yonemasu R, Yamamoto K and Yasui A, Characterization of a UV endonuclease gene from the fission yeast *Schizosaccharomyces pombe* and its bacterial homolog, *Nucleic Acids Res*. **24** (1996), pp. 1267-1271

Tanihigashi H, Yamada A, Igawa E and Ikeda S, The role of *Schizosaccharomyces pombe* DNA repair enzymes Apn1p and Uve1p in the base excision repair of apurinic/apyrimidinic sites, *Biochem. Biophys. Res. Commun*. **347** (2006), pp. 889-894

Taylor JS, Garrett DS and Cohrs MP, Solution-state structure of the Dewar pyrimidinone photoproduct of thymidylyl-(3'-5')-thymidine, *Biochemistry* **27** (1988), pp. 7206-7215

Theis K, Chen PJ, Skorvaga M, Van Houten B and Kisker C, Crystal structure of UvrB, a DNA helicase adapted for nucleotide excision repair, *EMBO J*. **18** (1999), pp. 6899-6907

Todo T, Kim S.-T, Hitomi K, Otoshi E, Inui T, Morioka H, Kobayashi H, Ohtsuka E, Toh H and Ikenaga M, Flavin adenine dinucleotide as a chromophore of the *Xenopus* (6-4) photolyase, *Nucleic Acids Res*. **257** (1997), pp. 764–768

Todo T, Ryo H, Yamamoto K, Toh H, Inui T, Ayaki H, Nomura T and Ikenaga M, Similarity among the *Drosophila* (6-4) photolyase, a human photolyase homolog, and the DNA photolyase-blue-light photoreceptor family, *Science* **272** (1996), pp. 109–112

Todo T, Functional diversity of the DNA photolyase/blue light receptor family, *Mutat. Res*. **434** (1999), pp. 89-97

Truglio JJ, Croteau DL, Van Houten B and Kisker C, Prokaryotic nucleotide exsion repair, the UvrABC system, *Chem. Rev*. **106** (2006), pp. 233–252.

Truglio JJ, Rhau B, Croteau DL, Wang L, Skorvaga M, Karakas E, DellaVecchia MJ, Wang H, Van Houten B and Kisker C, Structural Insights into the first incision reaction during nucleotide excision repair, *EMBO J*. **24** (2005), pp. 885-894

Van Houten B, Croteau DL, DellaVecchia MJ, Wang H and Kisker C, 'Close-fitting sleeves': DNA damage recognition by the UvrABC nuclease system, *Mutat. Res*. **577** (2005), pp. 92-117

Vassylyev G, Kashiwagi T, Mikami Y, Ariyoshi M and Iwai S, Atomic model of a pyrimidine dimer excision repair enzyme complexed with a DNA substrate: structural basis for damaged DNA recognition, *Cell* **83** (1995), pp. 773-782

Verhoeven EE, van Kesteren M, Moolenaar GF, Visse R and Goosen N, Catalytic sites for 3' and 5' incision of *Escherichia coli* nucleotide excision repair are both located in UvrC, *J. Biol. Chem*. **275** (2000), pp. 5120-5123

Verhoeven EE, Wyman C, Moolenaar GF and Goosen N, The presence of two UvrB subunits in the UvrAB complex ensures damage detection in both DNA strands, *EMBO J*. **21** (2002), pp. 4196-4205

Viadiu H and Aggarwal AK, The role of metals in catalysis by the restriction endonuclease *Bam*HI, *Nat*. *Struct*. *Biol*. **5** (1998), pp. 910-916

Wang CI and Taylor JS, Site-specific effect of thymine dimer formation on dAn.dTn tract bending and its biological implications, *Proc*. *Natl*. *Acad*. *Sci*. *USA*. **85** (1991), pp. 2558-2562

Weber S, Light-driven enzymatic catalysis of DNA repair: a review of recent biophysical studies on photolyase, *Biochim*. *Biophys*. *Acta* **1707** (2005), pp. 1-23

Westheimer FH, Why nature chose phosphates, *Science* **235** (1987), pp. 1173-1178

Wilson M and Thompson H, Life without DNA repair, *Proc*. *Natl*. *Acad*. *Sci*. *USA*. **94** (1997), pp. 12754-12757

Worthington E, Kavakli I, Berrocal-Tito G, Bondo B and Sancar A, Purification and characterization of three members of the photolyase/cryptochrome family blue-light photoreceptors from *Vibrio cholerae*, *J*. *Biol*. *Chem*. **278** (2003), pp. 39143-39154

Yasui A, Eker AP, Yasuhira S, Yajima H, Kobayashi T, Takao M and Oikawa A, A new class of DNA photolyases present in various organisms including aplacental mammals, *EMBO J*. **13** (2001), pp. 6143-6151

Yasui A and McCready SJ, Alternative repair pathways for UV-induced DNA damage, *Bioessays* **20** (1998), pp. 291-297

Yonemasu R, McCready SJ, Murray JM, Osman F, Takao M, Yamamoto K, Lehmann AR and Yasui A, Characterization of the alternative excision repair pathway of UV-damaged DNA in *Schizosaccharomyces pombe*, *Nucleic Acids Res*. **25** (1997), pp. 1553-1558

Yoon JH, Lee CS, O'Connor TR, Yasui A and Pfeifer GP, The DNA damage spectrum produced by simulated light, *J*. *Mol*. *Biol*. **299** (2000), pp. 681-693

Yoon JH, Swiderski PM, Kaplan BE, Takao M, Yasui A, Shen B and Pfeifer GP, Processing of UV damage in vitro by FEN-1 proteins as part of an alternative DNA excision repair pathway, *Biochemistry* **38** (1999), pp. 4809-4817

Zhao X, Liu J, Hsu DS, Zhao S, Taylor JS and Sancar A, Reaction mechanism of (6-4) photolyase, *J*. *Biol*. *Chem*. **272** (1997), pp. 32580-32590